ENERGY EFFICIENCY OF PLANAR DISCHARGE FOR INDUSTRIAL APPLICATIONS

Jakub Kelar*, Jan Čech, Pavel Slavíček

Dept. of Physical Electronics, Masaryk University, Kotlarska 2, 611 37 Brno, Czech Republic

* corresponding author: `jakub.kelar@gmail.com`

Abstract. Diffuse Coplanar Surface Barrier Discharge has proven its capabilities as an industry-ready plasma source for fast, in-line and efficient plasma treatment at atmospheric pressure. One parameter required by industry is energy efficiency of the device. In this paper, we present the energy efficiency of the whole plasma system, and we investigate possible sources of errors.

Keywords: dielectric barrier discharge; DCSBD; electrical efficiency; power estimation; error analysis.

1. Introduction

Diffuse Coplanar Surface Barrier Discharge (DCSBD) is a special type of dielectric barrier discharge [1] that uses a planar parallel arrangement of electrodes [2, 3] embedded in the ceramic plate dielectric barrier and a dielectric cooling oil. DCSBD is a non-isothermal discharge [4, 5] which is able to generate macroscopically homogeneous plasma at atmospheric pressure in air and also in other working gases (O_2, N_2, CO_2, H_2, H_2O, etc.) [6–8]. The planar geometry and the macroscopically homogeneous plasma generated as a thin plasma layer (approx. 0.3 mm) make DCSBD an appropriate plasma source for treating planar surfaces with roughness below approx. 1 mm. DCSBD has been used with positive results for treating of non-woven textiles [9], wood [10], silicon wafers [11], various foils and fibers [12–14], glass [7], metals [8] and bio-materials [15]. In the work presented here, the energy efficiency of DCSBD was estimated in order to improve the electrical circuit parameters of the DCSBD device, if necessary. The energy efficiency was determined as the ratio of the power-to-plasma estimate and the measured electric power consumption of the electric power supply unit. The power-to-plasma estimates were based on direct power integration from the current and voltage measurements. The energy efficiency was measured in the power range from 100 to 400 W. The oscilloscope parameters and the measurement set up were also investigated as possible sources of errors in power estimates.

2. Experimental Procedure

2.1. Discharge source

The DCSBD device can be used in various geometric configurations. The dielectric barrier can be a flat or bent plate of 96% alumina ceramic. The electrode system can consist of electrodes of various thicknesses or with various electrode gap widths. For the measurements presented here, the planar DCSBD device has flat dielectrics with electrodes 1.5 mm in thickness and 1 mm spacing between the electrodes. Fig. 1
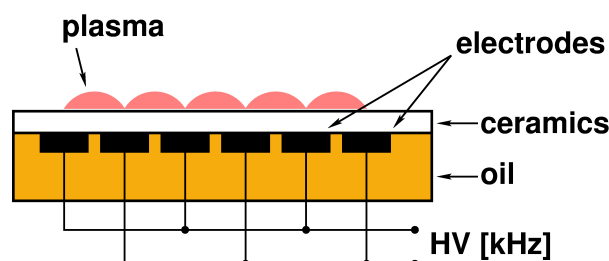

Figure 1. Simple scheme of the DCSBD device. Plasma layer, dielectric plate, cooling oil and electrodes on high voltage (HV).
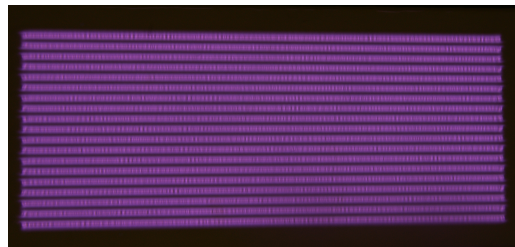

Figure 2. Image of DCSBD discharge generated in air at a power input of 400 W. The discharge area is about 8×20 cm^2.

shows the simplified cross-section of the DCSBD device. The periodic structure of high voltage (HV) and grounded electrodes as well as dielectric cooling oil and flat ceramic barrier are depicted.

The DCSBD discharge generated in air at atmospheric pressure and at an input power of 400 W at 15 kHz is given in Fig. 2. The visually homogeneous periodic structure of the discharge across the electrodes can be seen.

2.2. Electric parameters measurements and experimental set-up

For measurements of electrical efficiency of DCSBD two channel digital oscilloscope with a bandwidth of 100 MHz, maximal memory depth of 14 Mpts and sampling rate up to 2 GSa/s (Rigol DS2102) was used. For high voltage measurements the Tektronix P6015A
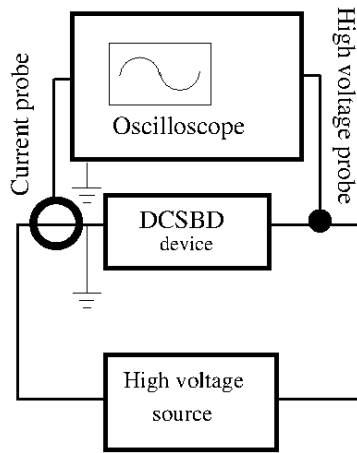
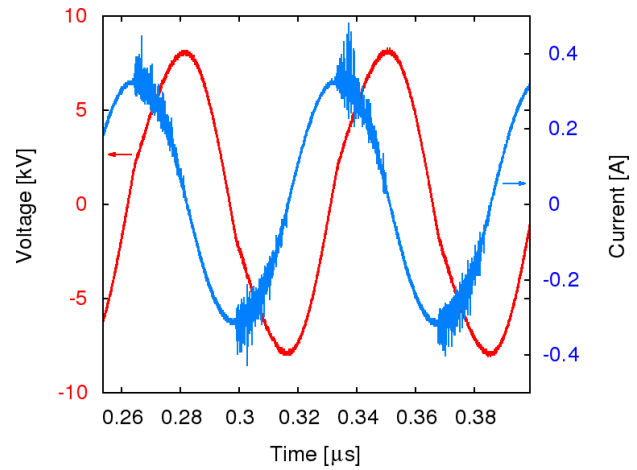FIGURE 3. Experimental set-up of DCSBD power efficiency measurement.

FIGURE 4. Typical current and voltage waveforms of DCSBD operated at input power of approx. 250 W.

FIGURE 5. Energy efficiency of the DCSBD device for selected input power of the power supply unit.

probe with 1:1000 ratio was used. The current probe Pearson current monitor 4100 with 1:1 ampere-to-volt ratio was used for current measurements. The simple scheme of experimental setup is given in Fig. 3.

3. RESULTS AND DISCUSSION

In this work the energy efficiency of a DCSBD device was calculated as the quotient of the measured high voltage power supply input power and the power-to-plasma estimated from high voltage and current measurements using direct power integration. A typical example of the current and voltage waveforms used for power-to-plasma estimation is given in Fig. 4. In Fig. 4 the capacitive and discharge currents (blue) can be distinguished.

The results of energy efficiency calculations are presented in Fig. 5. This calculation of power-to-plasma was performed using custom-made python or MATLAB script. The corresponding error of estimation, estimated from law of the error propagation, was determined to be approx. 6%.

In the process of DCSBD power-to-plasma estimation from current-voltage measurements, several sources of errors could be identified when the direct integration method is used. In this paper, three sources of errors are discussed using simulations in the MATLAB computational environment on the real measured data of a DCSBD discharge operated at an input power of 250 W (measured input power of the power supply unit).

The first source of errors was identified in the process of finding the zero-phase, i.e., the beginning of the discharge periods. The zero-phase of input voltage defines the interval of integration, so a false estimate could introduce a systematic power estimation error. In Fig. 6 the effect of zero-phase misalignment is shown on the y-axis. It can be seen that even 500 ns of zero-phase point misalignment does not induce significant errors of power-to-plasma estimation. This can be explained taking into account that the active
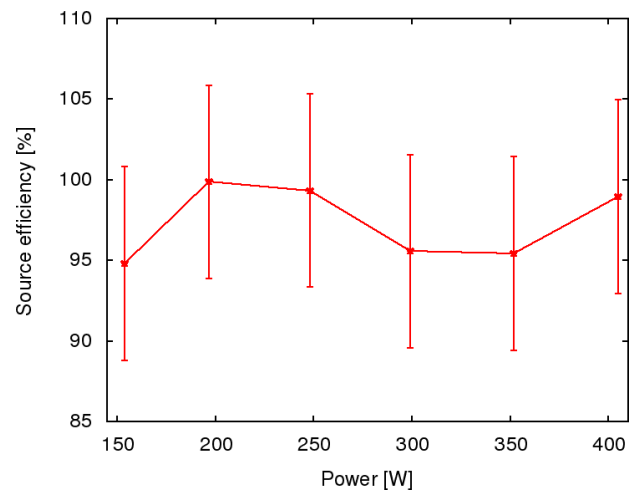
"discharge" phase starts at about the $\Pi/4$ phase of the input high voltage.

The second source of errors was identified in the current-voltage phase shift of the recorded waveforms. This phase shift could easily result from unequal length of the probe-to-scope cables, or from inaccurate oscilloscope parameters. Fig. 6 shows the effect of a current-voltage phase shift. It can be seen that this phase shift has a measurable effect on the estimated power-to-plasma value. A phase shift on the scale of several tens of ns shifts the estimated power input value by up to several tens of Watts. This effect can be explained by the capacitive coupling of the DCSBD. An ideal capacitor introduces a current-voltage phase shift of $\Pi/2$, so the real power over one period is zero. When the phase shift of current-voltage waveforms is introduced, a phase shift other than $\Pi/2$ occurs and the net integrated power consumption becomes non-zero.

A third source of errors was identified at the internal A/D converter of the oscilloscope – the precision, or the noise level of the sampled signal. This level
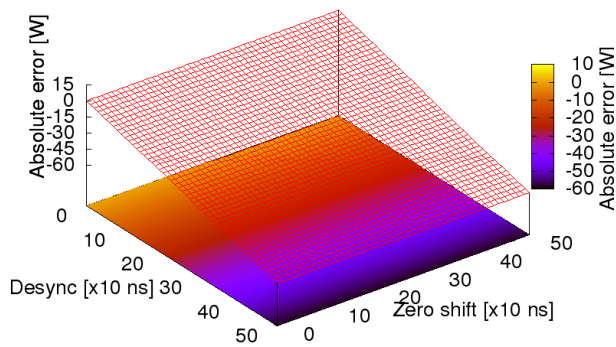
FIGURE 6. Absolute error of power-to-plasma/discharge power estimation using direct numerical integration of discharge current-voltage waveforms. The error of estimation resulting from a) a bad estimate of the beginning of the discharge period (labeled as 'zero shift' misalignment) and b) voltage-to-current waveform phase misalignment (i.e., voltage-current phase shift, labeled as 'desync') are given. The zero reference point (the origin) is given as the power estimated from raw measured data.

of conversion noise is inherent in each oscilloscope and cannot be lowered easily. In Fig. 7 the real current-voltage signal from the oscilloscope was salted with uniformly distributed pseudo-random noise of the magnitude of N bits of A/D converter resolution and then the input power was estimated. The average of 10 salted signal power estimates is used as a point in the graph. It can be seen that when high added noise is present the absolute error of the power input estimation can be more than 0 to 12 W at 250 W of input power (i.e., 5 % of the value).

From the results we can conclude that the power-to-plasma numeric estimation procedure is relatively robust. The artificially introduced current-voltage waveform distortions lead to relatively small errors in power estimation of the order of a few percent, even when relatively bad experimental conditions are assumed (i.e., phase shift < 50 ns and noise level < 2 bits). This error magnitude is comparable or less than the assumed measurement errors of current and voltage waveforms.

4. CONCLUSIONS

In the first part of the experiments presented here, the energy efficiency of the DCSBD device was calculated as the ratio of power-to-plasma and the input power of the power supply unit. Results have been given for DCSBD operated at a frequency of about 15 kHz and input power ranging from 100 to 450 W. We found that the DCSBD device has energy efficiency higher than 85 % in the given power input range. In the second part of our study, a power input of 250 W was chosen and the estimation of errors for power-to-
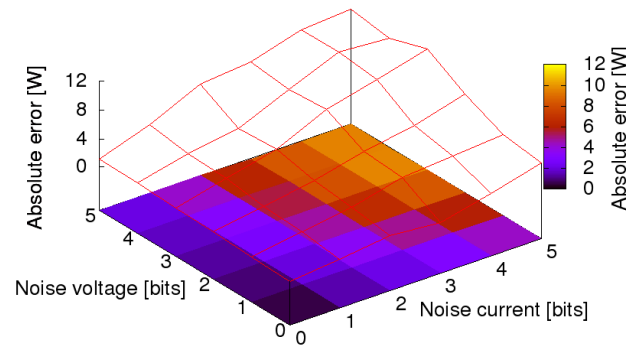

FIGURE 7. Absolute error of power-to-plasma/discharge power estimation using direct numerical integration of discharge current-voltage waveforms. The error of estimation due to the artificial noise (salt) added to the current and/or the voltage waveforms are visualized. The zero reference point (origin) is given as the power estimated from the raw measured data.

plasma were investigated using numerical simulations. The MATLAB computational environment was used to estimate the importance of making a precise calculation of the beginning of the discharge periods (zero-phase estimation), the influence of the phase shift of the voltage and current measurements, and the sensitivity of the process to the pseudorandom noise added to the real measured current and voltage waveforms. We have found that the power estimation process is relatively robust and stable, as the artificially induced power estimation errors were less than or equal to the assumed measurement errors, i.e., they were of the order of a few percent under a phase shift of < 50 ns and an added noise level of < 2 bits. The influence of zero-phase estimation was found to be negligible, provided that the phase misplacement is well below $\Pi/4$.

REFERENCES

[1] U. Kogelschatz. Dielectric-Barrier Discharges: Their History, Discharge Physics, and Industrial Applications. *Plasma chemistry and plasma processing* **23**(1):1–46, 2003. DOI:10.1023/A:1022470901385.

[2] M. Šimor, J. Rahel', P. Vojtek, et al. Atmospheric-pressure diffuse coplanar surface discharge for surface treatments. *Applied Physics Letters* **81**(15):2716, 2002. DOI:10.1063/1.1513185.

[3] V. I. Gibalov, G. J. Pietsch. Dynamics of dielectric barrier discharges in different arrangements. *Plasma Sources Science and Technology* **21**(2):024010, 2012. DOI:10.1088/0963-0252/21/2/024010.

[4] A. Fridman, A. Chirokov, A. Gutsol. Non-thermal atmospheric pressure discharges. *Journal of Physics D: Applied Physics* **38**(2):R1–R24, 2005. DOI:10.1088/0022-3727/38/2/R01.

[5] K. H. Becker, U. Kogelschatz, K. H. Schoenbach, R. J. Barker (eds.). *Non-Equilibrium Air Plasmas At Atmospheric Pressure.* Institute of Physics Publishing, Bristol, 2004.

[6] M. Černák, L. Černáková, I. Hudec, et al. Diffuse Coplanar Surface Barrier Discharge and its applications for in-line processing of low-added-value materials. *The European Physical Journal Applied Physics* **47**(2):22806, 2009. DOI:10.1051/epjap/2009131.

[7] T. Homola, J. Matoušek, V. Medvecká, et al. Atmospheric pressure diffuse plasma in ambient air for ITO surface cleaning. *Applied Surface Science* **258**(18):7135–7139, 2012. DOI:10.1016/j.apsusc.2012.03.188.

[8] V. Prysiazhnyi, A. Brablec, J. Čech, et al. Generation of Large-Area Highly-Nonequlibrium Plasma in Pure Hydrogen at Atmospheric Pressure. *Contributions to Plasma Physics* **54**(2):138–144, 2014. DOI:10.1002/ctpp.201310060.

[9] M. Černák, D. Kováčik, J. Ráhel', et al. Generation of a high-density highly non-equilibrium air plasma for high-speed large-area flat surface processing. *Plasma*

[10] J. Ráhel', P. Sťahel, M. Odrášková. Wood surface modification by dielectric barrier discharges at atmospheric pressure. *Chemické Listy* **105**(S2):S125–S128, 2011.

[11] D. Skácelová, V. Danilov, J. Schäfer, et al. Room temperature plasma oxidation in DCSBD: A new method for preparation of silicon dioxide films at atmospheric pressure. *Materials Science and Engineering: B* **178**(9):651–655, 2013. DOI:10.1016/j.mseb.2012.10.017.

[12] A. Asadinezhad, I. Novák, M. Lehocký, et al. An in vitro bacterial adhesion assessment of surface-modified medical-grade PVC. *Colloids and surfaces B, Biointerfaces* **77**(2):246–56, 2010. DOI:10.1016/j.colsurfb.2010.02.006.

[13] I. Hudec, M. Jasso, H. Krump, et al. The influence of plasma polymerization on adhesion of polyester cords to rubber matrix. *KGK-KAUTSCHUK GUMMI KUNSTSTOFFE* **61**(3):95–97, 2008.

[14] M. Stepankova, J. Saskova, J. Gregr, J. Wiener. USING OF DSCBD PLASMA FOR TREATMENT OF KEVLAR AND NOMEX FIBERS. *CHEMICKE LISTY* **102**(4, SI):S1515–S1518, 2008.

[15] M. Henselová, U. Slováková, M. Martinka, A. Zahoranová. Growth, anatomy and enzyme activity changes in maize roots induced by treatment of seeds with low-temperature plasma. *Biologia* **67**(3):490–497, 2012. DOI:10.2478/s11756-012-0046-5.

Physics and Controlled Fusion **53**(12):124031, 2011. DOI:10.1088/0741-3335/53/12/124031.